

TiO₂ nanotubes modified with cadmium oxide for photoelectrocatalytic oxidation of alcohols

Vitali A. Grinberg^a, Victor V. Emets^b, Aleksey V. Shapagin^c, Aleksey A. Averin^d, Andrei A. Shiryaev^e

Frumkin Institute of Physical Chemistry and Electrochemistry, Russian Academy of Sciences, Moscow, Russia

^avitgreen@mail.ru, ^bVictoremets@mail.ru, ^cshapagin@mail.ru, ^dalx.av@yandex.ru, ^ea_shiryaev@mail.ru

Corresponding author: Victor V. Emets, Victoremets@mail.ru

PACS 82.47.Jk

ABSTRACT TiO₂ nanotube (TNT) electrodes were fabricated by electrochemical anodization of titanium in ethylene glycol electrolyte with added NH₄F (0.5 wt.%) and water (2 % w/w). The (TNT)-cadmium oxide (CdO) composite was fabricated using potentiostatic cathodic deposition. Structural properties of the obtained coatings have been investigated by scanning electron microscopy and X-Ray photoelectron spectroscopy, Raman spectroscopy, X-Ray diffraction and transmission electron microscopy. The TNT-CdO electrode demonstrates high efficiency in photoelectrochemical degradation of methanol, ethylene glycol, glycerol and sorbitol in aqueous solutions of 0.1 M Na₂SO₄ upon irradiation by a simulated sunlight. The highest photooxidation currents were obtained for sorbitol. Intensity-modulated photocurrent spectroscopy shows that the photoelectrocatalysis efficiency is due to suppression of the electron-hole pairs' recombination and to increase in the rate of photo-induced charge transfer. Thus, the TNT-CdO composite is an effective photoanode for developing the technology of photoelectrochemical degradation of sorbitol and other alcohols by-products of biofuel production.

KEYWORDS Nanotubes, TiO₂-CdO composite, photoelectrocatalytic oxidation, methanol, ethylene glycol, glycerol, sorbitol

ACKNOWLEDGEMENTS This research was financially supported by the Ministry of Science and Higher Education of the Russian Federation and performed using the equipment of the Center for Collective Use of Physical Investigation Methods of the IPCE RAS.

FOR CITATION Grinberg V.A., Emets V.V., Shapagin A.V., Averin A.A., Shiryaev A.A. TiO₂ nanotubes modified with cadmium oxide for photoelectrocatalytic oxidation of alcohols. *Nanosystems: Phys. Chem. Math.*, 2025, **16** (3), 352–363.

1. Introduction

Titania – TiO₂ – is widely used in very diverse fields due to its high photosensitivity, non-toxicity, simplicity of preparation and stability in a wide pH range [1,2]. Rich variety of nanostructured titania morphologies may be fabricated, such as nanoparticles, nanotubes and nanofibers. Harvesting solar energy by titania nanotubes (TNT) prepared by titanium anodization [3, 4] attracts considerable attention due to higher rate of photogenerated charge transfer in comparison with films made of titania nanoparticles [5,6]. Large band gap of TiO₂ limits light absorption to photons with energies close to UV-range. Absorption in the visible spectral range is made possible by introducing dopants narrowing the band gap; for example, CdS [7, 8], CdSe [9, 10], TiSi₂ [11], Fe₂O₃ [12] and NiO [13]. In particular, admixture of CdO, a n-type semiconductor characterized by a 2.32 eV direct and 1.36 eV indirect band gaps [14], is promising for several applications. Nanostructured TNT-CdO materials could be obtained using different approaches including electrodeposition of CdO on TNT substrate [15] or soaking of TNT with cadmium salts with subsequent annealing in air [16]. These composites demonstrate noticeable enhancement of water photoelectrochemical oxidation relative to pure TNT.

Common approaches to decompose the alcohols into carbonyl compounds are characterized by harsh reaction conditions, formation of abundant harmful waste and low selectivity. Novel methods based on photo-, electro- and photoelectrocatalytic alcohols' oxidation to precursors and intermediates for production of pharmaceuticals and other substances [17] combined with simultaneous production of pure hydrogen are of considerable theoretical and applied interest. Among alcohols produced from renewable biomass sorbitol plays an important role due to possibility of its conversion into alkanes, methanol and hydrogen by reforming in aqueous medium [18–21]. Sorbitol also serves as a precursor for medications (e.g., isosorbide – a popular diuretic), polymers, solvents, fuel additives etc [22].

In this work we report influence of CdO promotion on photoelectrocatalytic activity of nanostructured titania photoanodes in reaction of selective photoelectrochemical sorbitol degradation under simulated Solar light. The photoanodes

were made by two-step anodisation of VT1-0 titanium alloy followed by cathodic deposition of CdO. Note that the current study does not address the composition of the products of photoelectrooxidation of the mentioned alcohols.

2. Experimental

2.1. Materials

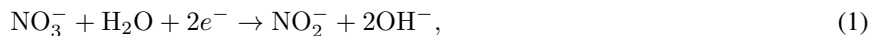
Chemically pure (>99 %) ammonium fluoride NH₄F and ethylene glycol (99.9 %), methanol, ethylene glycol, glycerol, sorbitol, Cd(NO₃)₂ · 4H₂O, sodium bicarbonate (NaHCO₃), sodium sulfate (Na₂SO₄) were purchased from (Aldrich, St. Louis, MO, USA) and used in the coating fabrication without further purification.

2.2. Preparation of TNT/Ti photoanodes

The electrodes were prepared by anodic oxidation of titanium foil (VT1-0 alloy, 99.5 % of Ti, 1.0 × 1.0 × 0.3 cm) at 20 °C in electrochemical cell, containing solution of ethylene glycol 0.5 % (w/w) NH₄F and 2 % (w/w) H₂O as supporting electrolyte, and a Pt–Ir plate (8 cm²) used as cathode. Two-step anodization procedure was employed to obtain stable and uniform structure [23–26]. The first step was performed at a constant voltage of 60 volts for 1 hour, followed by the coating removal in an ultrasonic bath in a 0.1 M HCl solution for 180 s. Next, the electrode was rinses with distilled water, air-dried at 50 °C and subjected to a second anodization step in the same solution at a constant voltage of 60 V for 1 hour. Subsequently, the TNT/Ti electrode was washed with deionized water, dried in air and annealed at 450 °C (heating rate 7 °C/min) for 1 h. After cooling in the oven for 12 h, the obtained samples coated with the uniform TNTs film were used for further investigations. The titania nanotubes grow due to two competitive reactions anodic oxidation and chemical dissolution of TiO₂ [27].

2.3. Preparation of TNT–CdO Photoanode

Cadmium oxide was deposited on the preformed TNT at a constant potential $E = -0.75$ V (vs. Ag/AgCl) from a 5 mM Cd(NO₃)₂ · 4H₂O + 0.1 M KCl solution while stirring the electrolyte according to the procedure described in [28]. Depending on the deposition time, the electric charge that passed varied between 50 and 800 mC. CdO formation via generation of intermediate Cd(OH)₂ was proposed in [29].



Cd(OH)₂ is converted to CdO at temperatures above 280 °C by the following reaction [30]:



2.4. Characterization of the TNT–CdO photoanodes

2.4.1. Study of the structure and phase composition of the TNT–CdO photoanodes. Morphology of the deposited TNT and TNT–CdO, the phase composition and Raman spectra were recorded as in [31–33].

Morphology of the deposited TNT and TNT–CdO was assessed by Scanning Electron Microscopy (SEM) with a JEOL JSM-6060 SEM and JED-2300 Analysis Station (JEOL).

The phase composition of the deposited film coatings was studied by X-ray diffraction (XRD) analysis on an Empyrean X-ray diffractometer (Panalytical BV). Ni-filtered Cu-K α radiation was used; the samples were studied in the Bragg–Brentano geometry. The phase composition was identified using the ICDD PDF-2 diffraction database.

Raman spectra were recorded using an inVia “Reflex” Raman spectrometer (Renishaw) with a 50× objective. The 405-nm line of a diode laser was used for excitation, and laser power on the sample was less than 0.2 mW.

XPS spectra were obtained on an OMICRON ESCA+ spectrometer (Germany) with an aluminum anode, equipped with a monochromatic X-ray source XM1000 (AlK α 1486.6 eV and a power of 252 W).

2.4.2. Photoelectrooxidation. Photoelectrochemical measurements were performed using a setup comprising photoelectrochemical three-electrode cell PECC-2 (Zahner Elektrik, Germany), a 150 W Solar spectrum simulator 96000 (Newport) with an AM1.5G filter, and an IPC-Pro MF potentiostat (IPChE RAS, Russia). The working electrode in the cell was a 1 cm² TNT and TNT–CdO photoanodes. A Pt wire with a surface area of approximately 3 cm² was used as an auxiliary electrode. All potentials are measured with a silver chloride electrode as a reference. Potentials relative to a reversible hydrogen electrode can be determined from the equation: $E_{\text{RHE}} = E_{\text{Ag/AgCl}} + 0.059 \times \text{pH} + E_{\text{Ag/AgCl}}$, where $E_{\text{Ag/AgCl}} = 0.197$.

Photoelectrochemical oxidation of alcohols (methanol, ethylene glycol, glycerol and sorbitol) and Intensity modulated photocurrent spectroscopy (IMPS) were carried out as described earlier in [31–33].

3. Results and discussion

Several photoanode samples were fabricated for research. The samples with pure titania nanotube coatings are designated as TNT. The photoanodes with modified TNT films are denoted as TNT-(0.05)CdO, TNT-(0.2)CdO, TNT-(0.8)CdO, where the number in parentheses denotes the electric charge spent on the electrodeposition of CdO in Coulombs per cm^2 of the geometric surface of the photoanode. The technique for manufacturing photoanode samples is described in detail in the Experimental details section.

Nanotubular structure of the TNT and TNT-CdO samples annealed at $450\text{ }^\circ\text{C}$ is clearly visible in scanning electron microscopy (SEM) images, see Fig. 1. The nanotubes are $20 - 22\ \mu\text{m}$ long, average wall thickness is $\sim 20\ \text{nm}$ and average diameter of nanotubes is $\sim 100\ \text{nm}$. Results of chemical analyses are shown in Fig. A1 and Tables A1–A4 (Appendix).

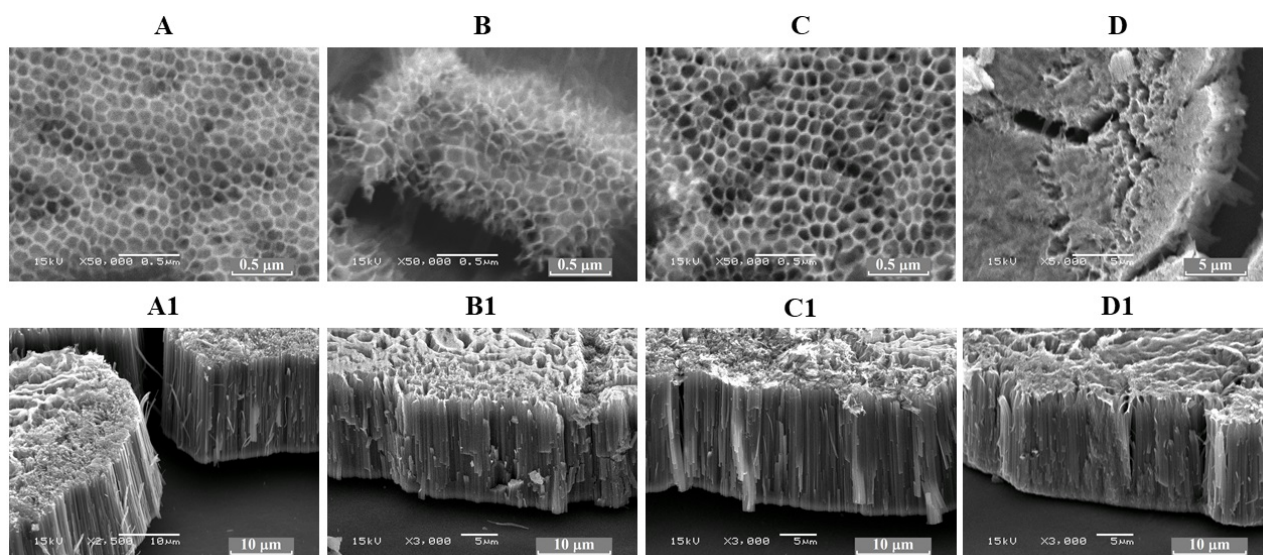


FIG. 1. SEM images (SE mode) of the TNT photoanodes obtained by two-stage titanium anodization (see text for detail). A – pure TNT film; B, C, D – CdO cathodically deposited with 50, 200 and 800 mC, respectively. Images A1, B1, C1, D1 were acquired at sample inclination of 45° relative to the incident electron beam

X-ray diffraction patterns and Raman spectra of the TNT-(0.05)CdO, TNT-(0.2)CdO, TNT-(0.8)CdO (Fig. 2) samples show absence of peaks due to CdO or CdTiO_3 . The patterns/spectra are virtually identical and correspond to the anatase polymorph of TiO_2 . The relative intensity of the 004 and 105 anatase reflections varies slightly between the samples, reflecting minor differences in texture of the deposited films. The 004 texture of the deposited TNT films is much less pronounced than in our previous study of the TNT-based photoanodes [33]. The only minor change in the Raman spectra is a slight decrease in intensity of the A_{1g} and of the B_{1g} peaks (517 and $395\ \text{cm}^{-1}$, respectively) relative to the E_g mode observable for the two samples with the highest amount of the deposited CdO. These variations are difficult to discuss quantitatively, but may also correspond to texture. Fig. 1(D and D1) demonstrate that at the highest electric charge (0.8 C) during the CdO electrodeposition the surface of the TNT becomes “smeared”, presumably, due to large amount of defects. Nevertheless, even in this sample separate Cd-rich phase are not formed. This implies formation of cadmium solid solution in titania.

Positions of Ti 2p transitions in X-ray photoelectron spectra correspond to anatase. Positions of the Cd $3d_{5/2}$ and $3d_{3/2}$ peaks (405.6 and 412.5 eV, respectively) are slightly higher than reported for CdO (e.g., compilation at <https://xpsdatabase.net/>, accessed on 13.11.2024), which implies lowering of the electron density on Cd ions, presumably, due to distortions of the TiO_2 -CdO solid solution lattice and/or presence of vacancies (Fig. A2, Appendix). The shift may be also related to electron transfer from Cd to Ti as suggested in [15].

Figure A3 (Appendix) shows TEM image of a carbon replica from the TNT-(0.2)CdO sample. The TNT array is covered by micron-size spherulites. Most likely, the formation of the spherulites results from incorporation of large amount of Cd impurity into anatase lattice. Note that texture, pronounced in spherulites, is also manifested in Raman spectra.

3.1. Photoelectrocatalytic degradation of methanol, ethylene glycol, glycerol and sorbitol aqueous solutions in $0.1\ \text{M}\ \text{Na}_2\text{SO}_4$

Figure 3A shows voltammograms of photoelectrochemical oxidation of water and of several alcohols on the prepared TNT photoanode. Addition of the alcohols into the aqueous solution shifts the photoanode potential towards the cathode

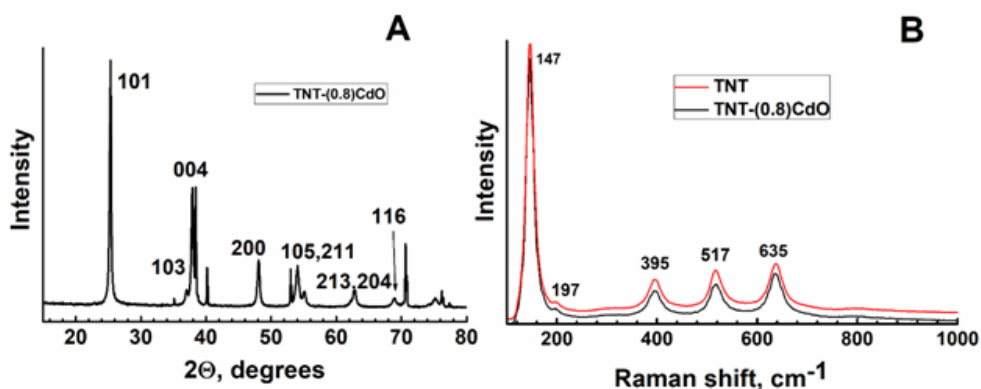


FIG. 2. Phase composition of the TNT-CdO samples after cathodic deposition of CdO. A – X-ray diffraction pattern, reflections of anatase are noted. Sharp peaks correspond to titanium substrate. B – the Raman spectrum of the initial TNT and of the TNT-(0.8)CdO sample, positions of the main anatase peaks are indicated. The curves are displaced vertically for clarity

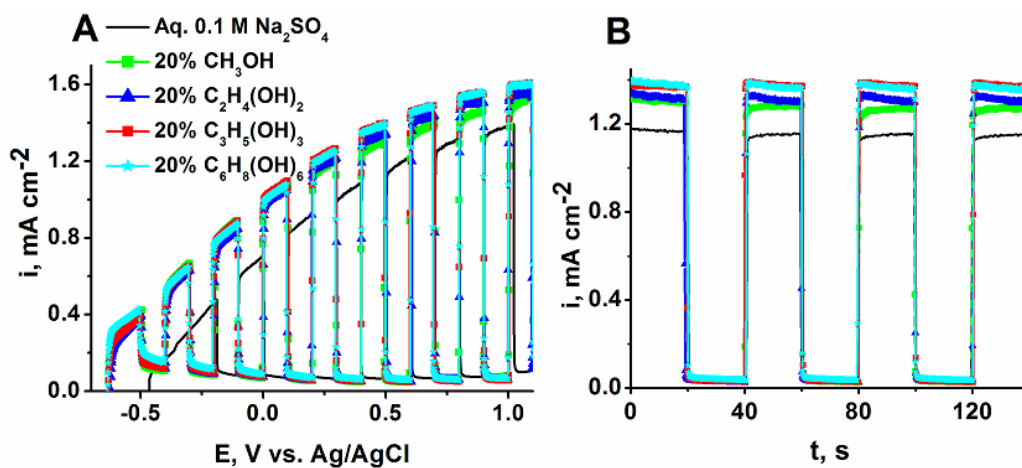


FIG. 3. Voltammetry of the TNT photoanode under the “light–dark” conditions. A – Voltammograms of the TNT photoanode; B – Photocurrent transients measured at $E = 0.5$ V (vs. Ag/AgCl). The background solution (black curve) corresponds to aqueous 0.1 M Na₂SO₄ solution. Other curves correspond to the background solution with 20 % addition of CH₃OH, C₂H₄(OH)₂, C₃H₅(OH)₃, C₆H₈(OH)₆, respectively. Illumination is performed by a sunlight simulator with a power density of 100 mW·cm⁻². Potential scan rate is 10 mV·s⁻¹

one; the oxidation photocurrents increase with the alcohol atomicity. Time-dependent transients of the oxidation photocurrents of water and of the alcohols on the TNT photoanode at a potential 0.5 V rel. Ag/AgCl (Fig. 3B) confirm the voltammetry results. The oxidation photocurrents of glycerin and sorbitol are virtually equal and are the highest (0.2 – 0.3 mA) among the studied compounds. This indicated that concentration of photogenerated holes reaches plateau and does not depend on number of hydroxyls (from 3 to 6) in the alcohol molecule.

Water photooxidation currents decrease in line with the increase of the CdO admixture to the TNT photoanode (Fig. 4A). This also follows from behavior of photocurrent transients (Fig. 4B), measured at a potential of 0.5 V relative to Ag/AgCl, as a function of the current spent for the Cd electrodeposition. Presumably, CdO admixture in TNT decreases the photoelectrocatalytic activity of the photoanode in oxidation of water molecules due to changes in rates of the relevant processes (recombination rate and rate of the charge transfer to a depolarizer molecule).

Earlier [31] we have shown that alcohol photoelectrooxidation current on an illuminated photoanode may correlate with number of alcohol structural groups. The highest photoelectrocatalytic currents were obtained for the sorbitol, the influence of the CdO modification of the TNT photoanodes is discussed on an example of this six-atomic alcohol. Fig. 5 shows that addition of 20 % (5.4 mM) of sorbitol into 0.1 M Na₂SO₄ solution leads to considerable increase of integral photoelectrocatalytic process on all CdO-promoted TNT photoanodes in comparison with water oxidation. The largest effect is observed for the TNT-(0.8)CdO photoanode. Fig. 6 reveals that the photoelectrooxidation currents for the six-atomic sorbitol and for one-atomic methanol are virtually equal, but the molar sorbitol concentration is approximately six times lower.

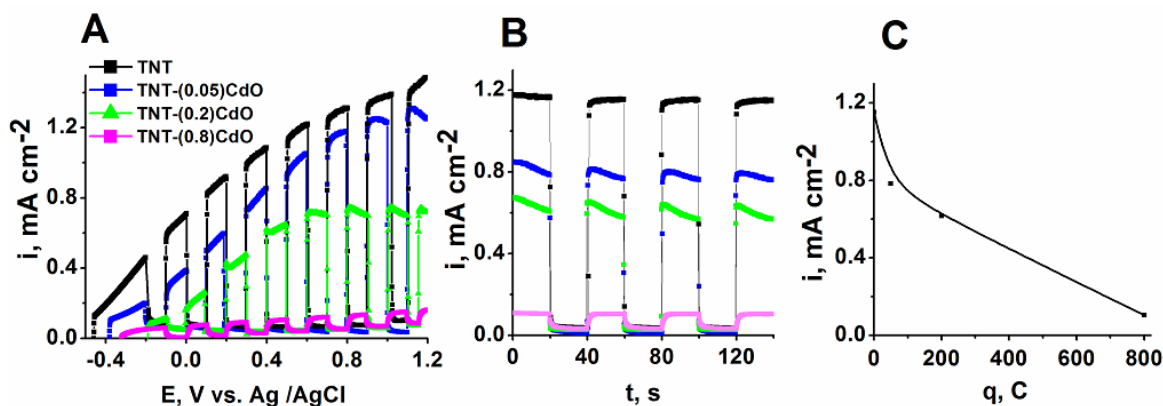


FIG. 4. Electrochemical measurements for the TNT-(x)CdO photoanodes under “light–dark” conditions in 0.1 M Na_2SO_4 aqueous solution. A – voltammograms curves; B – Photocurrent transients measured in 0.1 M Na_2SO_4 aqueous solution at $E = 0.5$ V (vs. Ag/AgCl); C – Dependence of the water photoelectrooxidation current at $E = 0.5$ V (vs. Ag/AgCl) as a function of the amount of deposited CdO

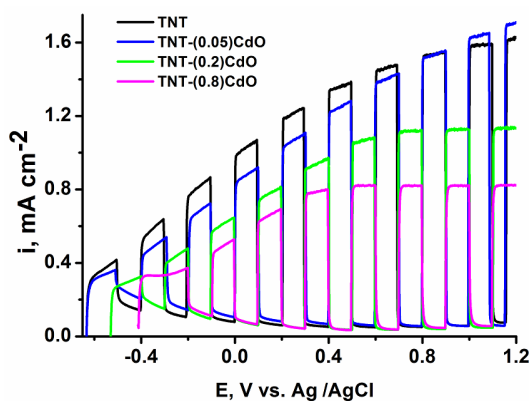


FIG. 5. Voltammograms under “light–dark” conditions in aqueous solution of 0.1 M Na_2SO_4 + 20 % $\text{C}_6\text{H}_8(\text{OH})_6$ for the photoanodes: TNT, TNT-(0.05)CdO, TNT-(0.2)CdO, TNT-(0.8)CdO

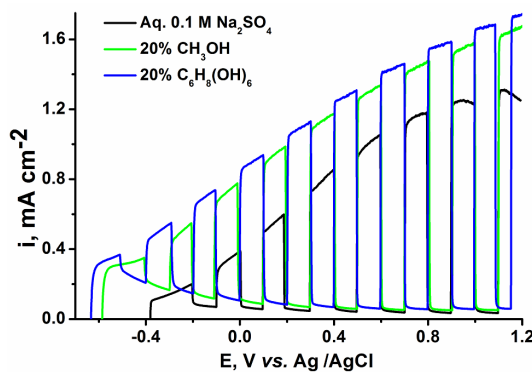


FIG. 6. Voltammograms of the TNT-(0.05)CdO photoanode under conditions “light–dark”. The background solution (black curve) is for the aqueous 0.1 M Na_2SO_4 solution. Other curves correspond to the background solution with 20 % addition of CH_3OH , $\text{C}_6\text{H}_8(\text{OH})_6$, respectively. Illumination is performed by a sunlight simulator with a power density of $100 \text{ mW}\cdot\text{m}^{-2}$. Potential scan rate is $10 \text{ mV}\cdot\text{s}^{-1}$

Even minimal admixture of CdO in TNT increases partial currents of sorbitol photoelectrooxidation at least two times in comparison with pure TNT photoanode. Transients of the photoelectrooxidation currents are shown in Fig. 7. The dependence of the sorbitol photoelectrocatalysis on amount of deposited Cd is shown in Fig. 8.

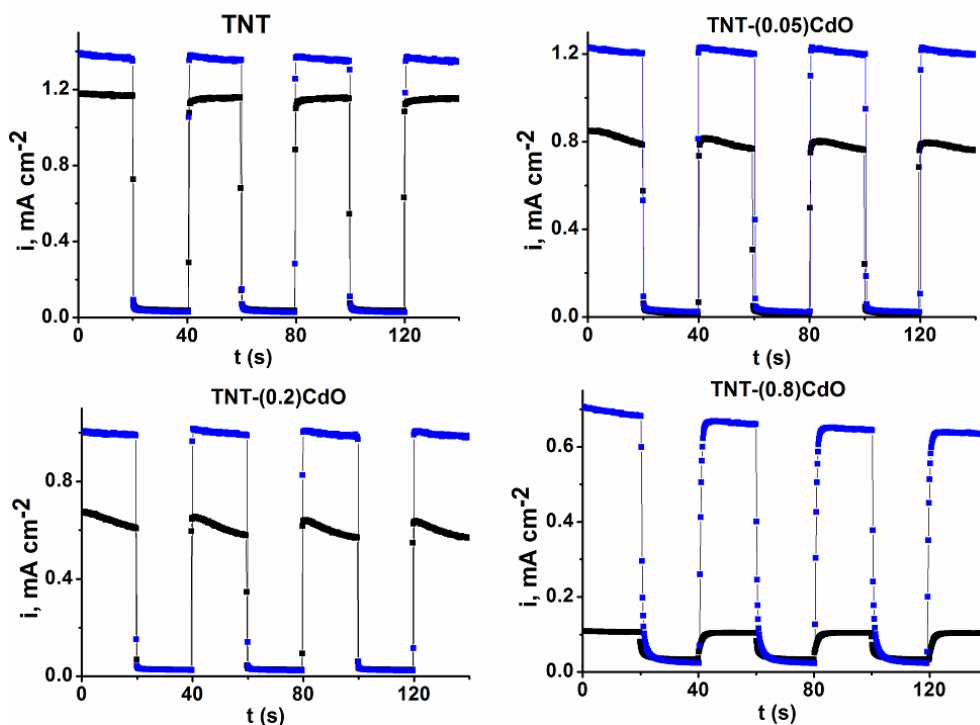


FIG. 7. Photocurrent transients measured in 0.1 M Na₂SO₄ aqueous solution with addition of 20 % of C₆H₈(OH)₆ at $E = 0.5$ V (vs. Ag/AgCl) for the TNT $-(x)$ CdO photoanodes. For all panels, the blue curve corresponds to the solution with added C₆H₈(OH)₆; the black curve – to the pure 0.1 M Na₂SO₄ solution

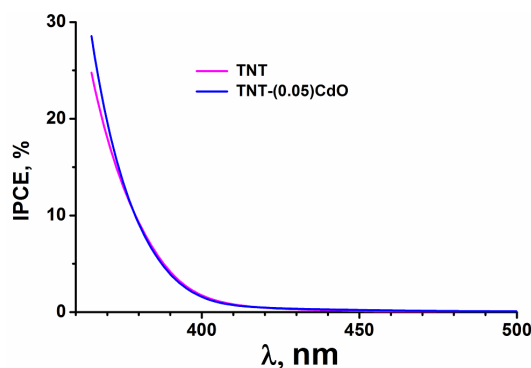


FIG. 8. Dependence of the partial current of photoelectrooxidation of 5.4 mM C₆H₈(OH)₆ at $E = 0.5$ V (vs. Ag/AgCl) on the amount of deposited CdO

3.2. Estimation of recombination losses in the photoelectrooxidation of sorbitol

Figure A4 (Appendix) shows wavelength dependence of incident photon to current efficiency (IPCE %) for the TNT and TNT-(0.05)CdO photoanodes in 0.1 M Na₂SO₄ aqueous solution. The sharp rise of the photocurrent is observed below ~ 400 nm, which is consistent with crystalline anatase. Formation of the solid solution upon Cd addition does not shift neither the IPCE, nor the optical absorption spectra (relative to pure anatase in the latter case).

Recombination losses of photogenerated holes in the TNT photoanode in course of water and sorbitol photooxidation were studied using Intensity-modulated photocurrent spectroscopy (IMPS) [34–36]. Monochromatic light with wavelength of 385 nm ($8 \text{ mW} \cdot \text{cm}^{-2}$ power density) was selected since it corresponds to IPCE % values (Fig. 9), providing sufficient precision of the IMPS measurements. The IMPS spectra were obtained in 0.1 M Na₂SO₄ and in 0.1 M Na₂SO₄ + 5.4 mM sorbitol solutions at 0.2 V potential. The high frequency intercept of the IMPS curve with the abscissa gives total

amount of photogenerated current I_2 . The low-frequency part gives I_1 , corresponding to oxidation of compounds present in the electrolyte. For the 0.1 M Na_2SO_4 solution, high curvature of the IMPS trace in the first quadrant at low modulation frequency (Fig. 9A) points to recombination losses at the TNT photoanode in course of water oxidation. Subsequently, $I_1 < I_2$. Sorbitol addition markedly increases I_2 value (the radius of the IMPS semi-circle increases). Larger I_2 values reflect higher oxidation rate of sorbitol in comparison with water; weak bending of the IMPS curve in the first quadrant suggests lower recombination losses.

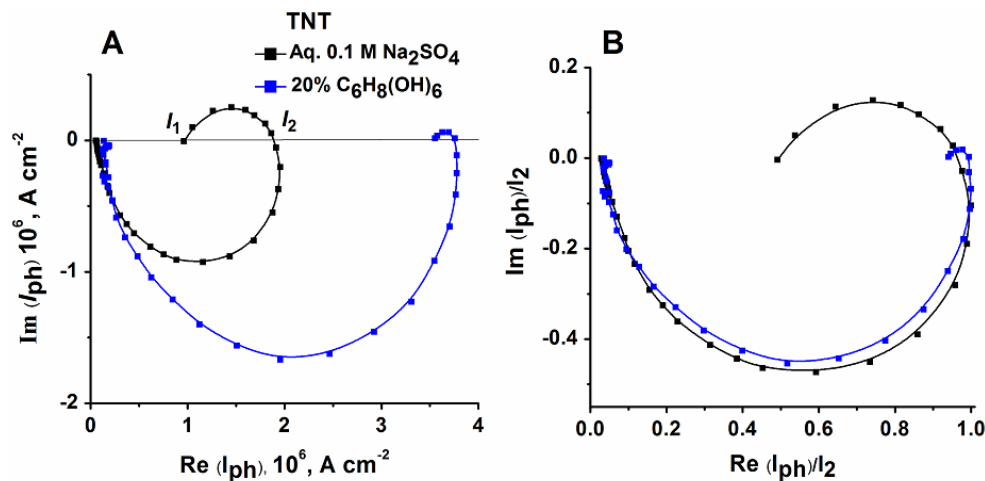


FIG. 9. IMPS (A) and normalized IMPS (B) dependences measured at $E = 0.2$ V (vs. Ag/AgCl) on the TNT photoanode. Illumination is performed by monochromatic 385 nm light, $8 \text{ mW}\cdot\text{cm}^{-2}$ power density

For quantitative analysis, the IMPS curves were normalized to I_2 (Fig. 9). In 0.1 M Na_2SO_4 at $E = 0.2$ V, the water oxidation photocurrent reaches 50 % of the total photogenerated current, $I_1/I_2 = 0.5$ (Fig. 9B, black curve); the recombination losses are also ~ 50 %, $(I_2 - I_1)/I_2 = 0.5$. Addition of 5.4 mM of sorbitol reduces the losses to ~ 7 % (Fig. 9B, blue curve), since higher photooxidation rate of sorbitol consume the holes from surface states of the TNT photoanode.

The IMPS measurements allow estimation of the recombination rate constant K_{rec} and charge transfer constant K_{ct} . The I_1/I_2 ratio of the low frequency part of the IMPS spectrum is related to these constants as $I_1/I_2 = K_{\text{ct}}/(K_{\text{rec}} + K_{\text{ct}})$. The frequency of the light intensity in the semi-circle maximum in the first quadrant (f_{max}) is related to K_{rec} and K_{ct} by the equation $2\pi f_{\text{max}} = (K_{\text{rec}} + K_{\text{ct}})$. In case of water photoelectrooxidation on the TNT photoanode at $E = 0.2$ V the calculated values of K_{ct} and K_{rec} are 0.247 and 0.247 s^{-1} , respectively. For the sorbitol photoelectrooxidation $K_{\text{ct}} = 0.46 \text{ s}^{-1}$ and $K_{\text{ct}} \gg K_{\text{rec}} = 0.034 \text{ s}^{-1}$; thus, sorbitol is more efficient acceptor of the photogenerated holes than water molecules.

Figure 10 shows that even minute admixture of Cd in the titania nanotubes leads to marked decrease of the recombination losses (there is no bend in the IMPS in the first quadrant at low modulation frequency). This observation is in line with increase of partial photocurrents of sorbitol oxidation on the Cd-promoted anode in comparison with the pure TNT photoanode (Fig. 7). Consequently, a photoanode based on Cd-promoted titania nanotubes is an efficient photoelectrocatalyser of sorbitol degradation. Presumably, the enhancement of this photoanode properties is due to small recombination losses of the photogenerated charges ($K_{\text{rec}} \ll 0.034 \text{ s}^{-1}$) and higher charge transfer rate ($K_{\text{ct}} > 0.46 \text{ s}^{-1}$) to a stronger acceptor.

Modification of TNT with CdO markedly increases sorbitol photoelectrooxidation rate both because of the smaller recombination constant and due to larger constant of the charge transfer to more efficient holes acceptor. Therefore, CdO-modified photoanodes from titania nanotubes may be employed for photoelectrochemical degradation of sorbitol and of other alcohols, by-products of biofuel manufacturing.

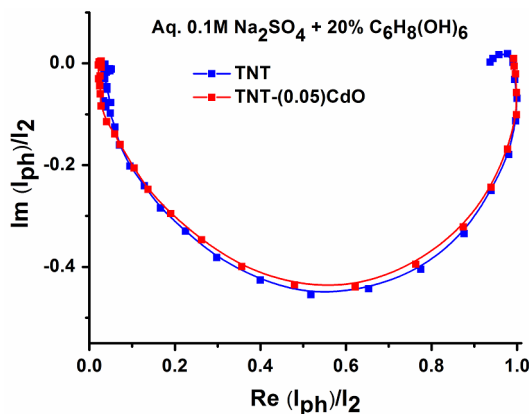


FIG. 10. IMPS dependences measured at $E = 0.2$ V (vs. Ag/AgCl) on the TNT and TNT-(0.05)CdO photoanodes in aqueous 0.1 M Na₂SO₄ with 20 % addition of C₆H₈(OH)₆. Illumination is performed by monochromatic 385 nm light, 8 mW·cm⁻² power density

4. Conclusions

Nanostructured photoanodes consisting of titania (anatase) nanotubes on a titanium substrate were fabricated by electrochemical anodization of Ti metal foil in ethylene glycol with addition of 0.5 wt.% NH₄F and 2 wt.% of water. Subsequently, various amounts of CdO were electrochemically deposited. At the employed conditions solid solutions CdO-TiO₂ were formed. Under illumination with solar light simulator, obtained photoanodes demonstrate high activity in photoelectrochemical degradation of alcohols, and, in particular, of sorbitol (C₆H₈(OH)₆) in aqueous 0.1 M Na₂SO₄ solution. The photoactivity increases with amount of CdO in the photoanode. Results of intensity-modulated photocurrent spectroscopy show that despite significant reduction in recombination losses due to formation of the CdO-TiO₂ solid solution, rate of water oxidation drops, presumably due to decrease of the charge transfer constant to H₂O molecules.

Appendix

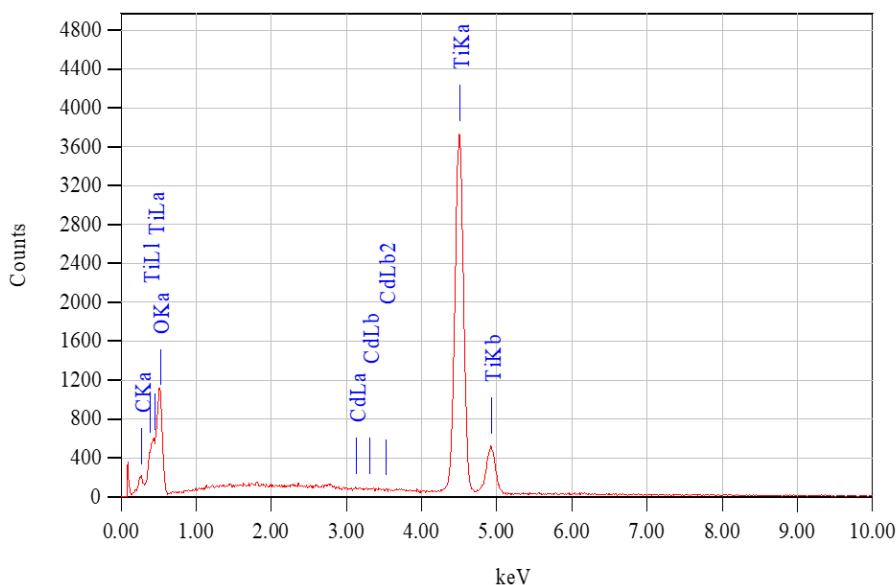


FIG. A1. Typical EDX spectrum of the samples TiO₂-NTbs promoted by CdO and Standardless Quantitative Analysis of samples with different cadmium oxide content presented in the Tables A1-A3

TABLE A1. ZAF Method Standardless Quantitative Analysis (0.05 C). Fitting Coefficient: 0.2626

Element	(keV)	Mass %	Error %	At % Compound	Mass % Cation K
C K	0.277	1.97	0.05	4.73	1.2149
O K	0.525	30.27	0.47	54.57	12.6515
Ti K	4.508	67.46	0.34	40.63	85.7918
Cd L*	3.132	0.30	0.47	0.08	0.3418
Total		100.00		100.00	

TABLE A2. ZAF Method Standardless Quantitative Analysis (0.2 C). Fitting Coefficient: 0.2679

Element	(keV)	Mass %	Error %	At % Compound	Mass % Cation K
C K	0.277	2.17	0.05	5.02	1.3691
O K	0.525	33.10	0.43	57.51	14.6929
Ti K	4.508	64.45	0.33	37.40	83.6111
Cd L*	3.132	0.28	0.46	0.07	0.3269
Total		100.00		100.00	

TABLE A3. ZAF Method Standardless Quantitative Analysis (0.8 C). Fitting Coefficient: 0.2617

Element	(keV)	Mass %	Error %	At % Compound	Mass % Cation K
C K	0.277	1.62	0.05	3.91	1.0134
O K	0.525	30.89	0.45	55.88	13.1659
Ti K	4.508	65.86	0.33	39.79	83.9665
Cd L*	3.132	1.62	0.46	0.42	1.8542
Total		100.00		100.00	

TABLE A4. Binding energy and the composition of the sample TiO₂-NTbs promoted by cadmium oxide (0.2 C/cm²)

Peak name		Eb, eV	Quant., at. %	
Ti2p	TiO ₂	459	25.95	25.95
Cd3d	Cd	405.6	0.12	0.12
	H ₂ O	533	3.36	
O1s	C-O	531.8	10.81	73.93
	C=O	531	7.9	
	TiO ₂	530.2	51.86	

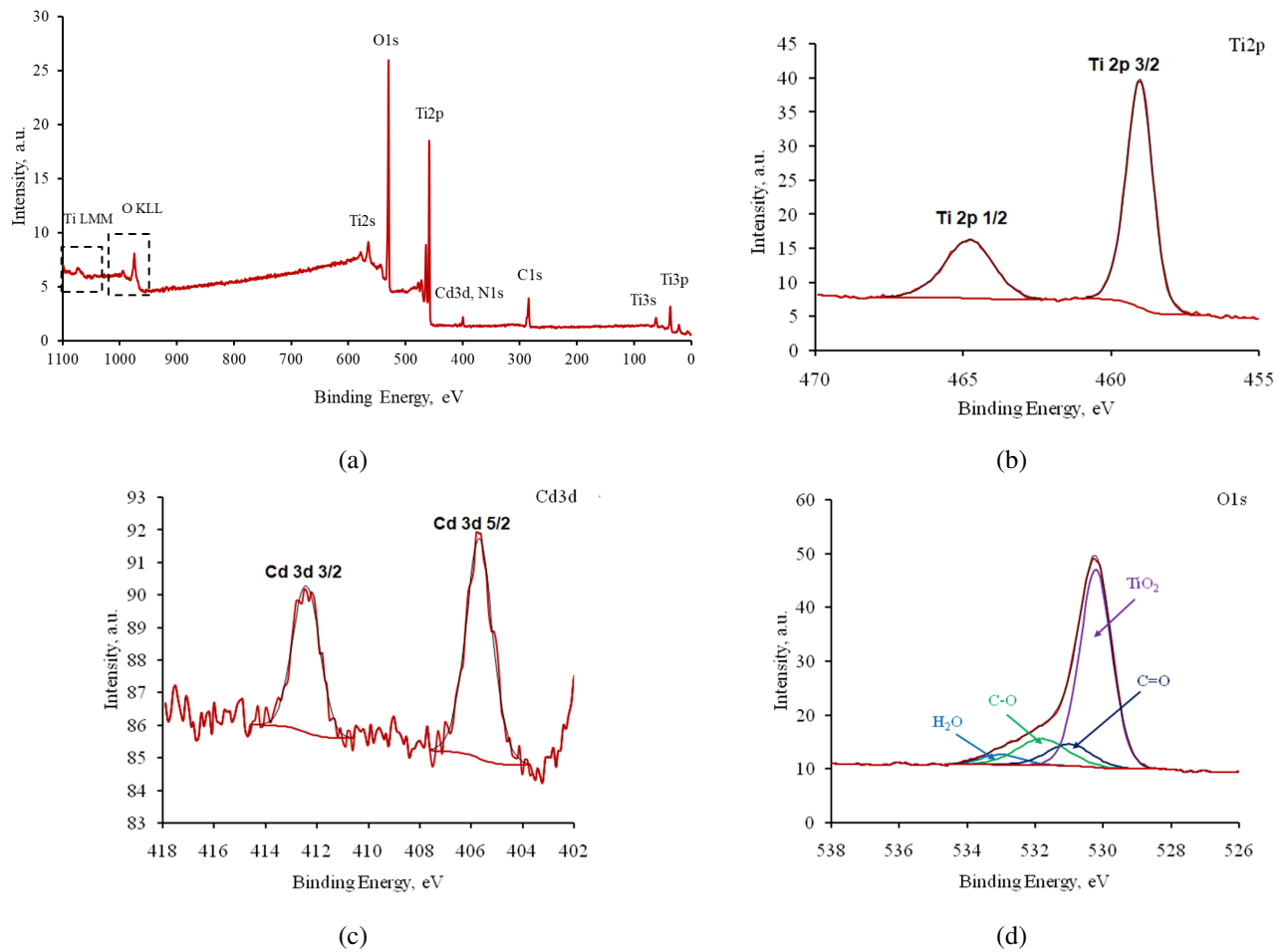


FIG. A2. XPS spectra of cadmium-modified TiO₂-NTBs prepared by cathodic deposition of CdO (0.2 C/cm²) (a); High-resolution XPS spectra of Ti 2p, Cd 3d and O 1s (b–d). The sample was calcined at 450 °C in air for 1 h

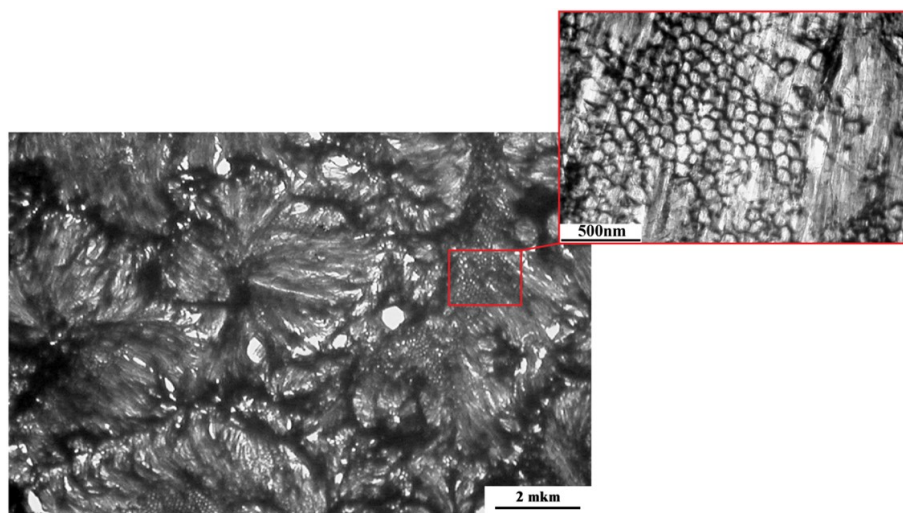


FIG. A3. TEM image of the supermolecular surface structure of TNT-(0.2)CdO

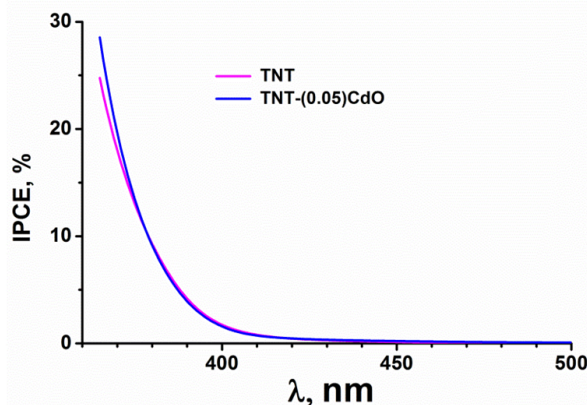


FIG. A4. Wavelength dependence of IPCE% for the TNT and TNT-(0.05)CdO photoanodes in 0.1 M Na_2SO_4 aqueous solution

References

- [1] Xia Y., Yang P., Sun Y., Wu Y., Mayers B., Gates B., et al. One-dimensional nanostructures: synthesis, characterization, and applications. *Adv. Mater.*, 2003, **15**, P. 353–389.
- [2] Banerjee S., Mohapatra S.K., Das P.P., Misra M. Synthesis of coupled semiconductor by filling 1D TiO_2 nanotubes with CdS. *Chem Mater.*, 2008, **20**, P. 6784–6791.
- [3] Zwilling V., Darque-Ceretti E., Boutry-Forveille A., David D., Perrin M.Y., Aucouturier M. Structure and physicochemistry of anodic oxide films on titanium and TA6V alloy. *Surf. Interface Anal.*, 1999, **27**, P. 629–637.
- [4] Gong D., Grimes C.A., Varghese O.K., Hu W., Singh R.S., Chen Z., et al. Titanium oxide nanotube arrays prepared by anodic oxidation. *J. Mater. Res.*, 2001, **16** (12), P. 3331–3334.
- [5] Mohapatra S.K., Misra M., Mahajan V.K., Raja K.S. Design of a highly efficient photoelectrolytic cell for hydrogen generation by water splitting: Application of $\text{TiO}_{2-x}\text{C}_x$ nanotubes as a photoanode and Pt/ TiO_2 nanotubes as a Cathode. *The J. of Physical Chemistry C*, 2007, **111** (24), P. 8677–8685.
- [6] Roy P., Berger S., Schmuki P. TiO_2 Nanotubes: Synthesis and Applications. *Angew. Chem. Int. Ed.*, 2011, **50**, P. 2904–2939.
- [7] Smith Y.R., Subramanain V. Heterostructural Composites of TiO_2 Mesh– TiO_2 Nanoparticles Photosensitized with CdS: A New Flexible Photoanode for Solar Cells. *J. Phys. Chem. C*, 2011, **115**, P. 8376–8385.
- [8] Liu Y., Zhou H., Zhou B., Li J., Chen H., Wang, J., et al. Highly stable CdS-modified short TiO_2 nanotube array electrode for efficient visible-light hydrogen generation. *Int. J. Hydrogen Energy*, 2011, **36**, P. 167–174.
- [9] Kongkanand A., Tvrdy K., Takechi K., Kuno M., Kamat P.V. Quantum Dot Solar Cells. Tuning Photoresponse through Size and Shape Control of CdSe– TiO_2 Architecture. *J. Am. Chem. Soc.*, 2008, **130**, P. 4007–4015.
- [10] Hossain M.F., Biswas S., Zhang Z.H., Takahashi T. Bubble-like CdSe nanoclusters sensitized TiO_2 nanotube arrays for improvement in solar cell. *J. Photochem. Photobiol. A: Chem.*, 2011, **217**, P. 68–75.
- [11] Banerjee S., Mohapatra S.K., Misra M. Water Photooxidation by TiSi_2 – TiO_2 Nanotubes. *J. Phys. Chem. C*, 2011, **115** (25), P. 12643–12649.
- [12] Mohapatra S.K., Banerjee S., Misra M. Synthesis of $\text{Fe}_2\text{O}_3/\text{TiO}_2$ nanorod–nanotube arrays by filling TiO_2 nanotubes with Fe. *Nanotechnology*, 2008, **19**, 315601.
- [13] Shrestha N.K., Yang M., Nah Y.-C., Paramasivam I., Schmuki P. Self-organized TiO_2 nanotubes: Visible light activation by Ni oxide nanoparticle decoration. *Electrochem. Commun.*, 2010, **12**, P. 254–257.
- [14] Dong W., Zhu C. Optical properties of surface-modified CdO nanoparticles. *Opt. Mater.*, 2003, **22**, P. 227–233.
- [15] Sarma B., Smith Y., Mohanty S.K., Misra M. Electrochemical deposition of CdO on anodized TiO_2 nanotube arrays for enhanced photoelectrochemical properties. *Materials Letters*, 2012, **85**, P. 33–36.
- [16] Wang X., Cheng K., Dou S., Chen Q., Wang J., Song Z., Zhang J., Song H. Enhanced photoelectrochemical performance of CdO– TiO_2 nanotubes prepared by direct impregnation. *Applied Surface Science*, 2019, **476**, P. 136–143.
- [17] Tang D., Lu G., Shen Z., Hu Y., Yao L., Li B., Zhao G., Peng B., Huang X. A review on photo-, electro- and photoelectro- catalytic strategies for selective oxidation of alcohols. *J. of Energy Chemistry*, 2023, **77**, P. 80–118.
- [18] Ruppert A.M., Weinberg K., Palkovits R. Hydrogenolyse goes Bio: Von Kohlenhydraten und Zuckerkohlen zu Plattformchemikalien. *Angew. Chem.*, 2012, **124**, P. 2614–2654.
- [19] Cortright R.D., Davda R.R., Dumesic J.A. Hydrogen from catalytic reforming of biomass-derived hydrocarbons in liquid water. *Nature*, 2002, **418**, P. 964–967.
- [20] Metzger J.O. Production of Liquid Hydrocarbons from Biomass. *Angew. Chem. Int. Ed.*, 2006, **45**, P. 696–698.
- [21] Huber G.W., Shabaker J.W., Dumesic J.A. Raney Ni–Sn Catalyst for H_2 Production from Biomass-Derived Hydrocarbons. *Science*, 2003, **300**, P. 2075–2077.
- [22] de Almeida R.M., Li J., Nederlof C., O’Connor P., Makkee M., Moulijn J.A. Cellulose Conversion to Isosorbide in Molten Salt hydrate Media. *ChemSusChem*, 2010, **3**, P. 325–328.
- [23] Zhang Z., Wang P. Optimization of photoelectrochemical water splitting performance on hierarchical TiO_2 nanotube arrays. *Energy Environ Sci.*, 2012, **5**, P. 6506–6512.
- [24] Kim H.I., Monllor-Satoca D., Kim W., Choi W. N-doped TiO_2 nanotubes coated with a thin TaO_xN_y layer for photoelectrochemical water splitting: dual bulk and surface modification of photoanodes. *Energy Environ Sci.*, 2015, **8**, P. 247–257.
- [25] Denisenko A.V., Morozov A.N., Michailichenko A.I. Obtaining coating consisting of nanotubes TiO_2 by anodizing the titanium in the electrolyte with an ethylene glycol with addition various amounts of water. *Adv. Chem & Chem. Techn.*, 2015, **29** (3), P. 71–73.

- [26] Ghicov A., Schmuki P. Self-Ordering Electrochemistry: A Review on Growth and Functionality of TiO₂ Nanotubes and Other Self-Aligned MO_x Structures. *Chemical Communications*, 2009, **45**, P. 2791–2808.
- [27] Robin A., de Almeida Ribeiro M.B., Rosa J.L., Nakazato R.Z., Silva M.B. Formation of TiO₂ nanotube layer by anodization titanium in ethylene glycol-H₂O electrolyte. *J. Surf. Eng. Mater. & Adv. Techn.*, 2014, **41**, P. 23–130.
- [28] Grinberg V.A., Emets V.V., Modestov A.D., Averin A.A., Shiryaev A.A. Thin-Film Nanocrystalline Zinc Oxide Photoanode Modified with CdO in Photoelectrocatalytic Degradation of Alcohols. *Coatings*, 2023, **13**, 1080.
- [29] Santamaria M., Bocchetta P., Quarto F.D. Room temperature electrodeposition of photoactive Cd(OH)₂ nanowires. *Electrochem. Commun.*, 2009, **11**, P. 580–584.
- [30] Gujar T.P., Shinde V.R., Kim W.Y., Jung K.D., Lokhande C.D., Joo O.S. Formation of CdO films from chemically deposited Cd(OH)₂ films as a precursor. *Appl. Surf. Sci.*, 2008, **254**, P. 3813–3818.
- [31] Grinberg V.A., Emets V.V., Mayorova N.A., Averin A. A., Shiryaev A.A. Photoelectrocatalytic Activity of ZnO-Modified Hematite Films in the Reaction of Alcohol Degradation. *Int. J. Mol. Sci.*, 2023, **24** (18), 14046.
- [32] Grinberg V.A., Emets V.V., Mayorova N.A., Averin A.A., Shiryaev A.A. Sn-Doped Hematite Films as Photoanodes for Photoelectrochemical Alcohol Oxidation. *Catalysts*, 2023, **13** (11), 1397.
- [33] Grinberg V.A., Emets V.V., Shapagin A.V., Averin A.A., Shiryaev A.A. Effect of the length of TiO₂ nanotubes on the photoelectrochemical oxidation of phenylacetic acid anions. *J. of Solid State Electrochemistry*, 2024, **29** (2), P. 629–638.
- [34] Peter L.M., Ponomarev E.A., Fermin D.J. Intensity-modulated photocurrent spectroscopy: Reconciliation of phenomenological analysis with multistep electron transfer mechanisms. *J. Electroanal. Chem.*, 1997, **427**, P. 79–96.
- [35] Peter L.M., Wijayantha K.G.U., Tahir A.A. Kinetics of light-driven oxygen evolution at a-Fe₂O₃ electrodes. *J. Faraday Discuss.*, 2012, **155**, P. 309–322.
- [36] Klotz D., Ellis D.S., Dotana H., Rothschild A. Empirical in operando Analysis of the Charge Carrier Dynamics in Hematite Photoanodes by PEIS, IMPS and IMVS. *J. Phys. Chem. Chem. Phys.*, 2016, **18**, P. 23438–23457.

Submitted 21 January 2025; revised 6 March 2025; accepted 5 May 2025

Information about the authors:

Vitali A. Grinberg – Frumkin Institute of Physical Chemistry and Electrochemistry, Russian Academy of Sciences, Laboratory of processes in chemical current sources, Leninsky Prospekt 31, Building 4, 119071 Moscow, Russia; ORCID 0000-0003-3223-3194; vitgreen@mail.ru

Victor V. Emets – Frumkin Institute of Physical Chemistry and Electrochemistry, Russian Academy of Sciences, Electrocatalysis laboratory, Leninsky Prospekt 31, Building 4, 119071 Moscow, Russia; ORCID 0000-0003-2746-449X; Victoremets@mail.ru

Aleksey V. Shapagin – Frumkin Institute of Physical Chemistry and Electrochemistry, Russian Academy of Sciences, Laboratory of structural and morphological research, Leninsky Prospekt 31, Building 4, 119071 Moscow, Russia; ORCID 0000-0002-8866-0710; shapagin@mail.ru

Aleksey A. Averin – Frumkin Institute of Physical Chemistry and Electrochemistry, Russian Academy of Sciences, Laboratory of new physical and chemical problems, Leninsky Prospekt 31, Building 4, 119071 Moscow, Russia; ORCID 0000-0003-2895-8539; alx.av@yandex.ru

Andrei A. Shiryaev – Frumkin Institute of Physical Chemistry and Electrochemistry, Russian Academy of Sciences, Laboratory of new physical and chemical problems, Leninsky Prospekt 31, Building 4, 119071 Moscow, Russia; ORCID 0000-0002-2467-825X; a_shiryaev@mail.ru

Conflict of interest: the authors declare no conflict of interest.